journal

J. Am. Ceram. Soc., 91 [5] 1572–1579 (2008)
DOI: 10.1111/j.1551-2916.2008.02309.x

Grain Growth Behavior of Bi_2O_3-Doped ZnO Grains in a Multilayer Varistor

Shu-Ting Kuo and Wei-Hsing Tuan*,†

Department of Materials Science and Engineering, National Taiwan University, Taipei, Taiwan 106

Yeh-Wu Lao, Chung-Kai Wen, and Huey-Ru Chen

Walsin Technology Corporation, Kaohsiung, Taiwan 700

A novel bismuth-doped zinc oxide (ZnO) laminated structure is prepared in the present study. Seven layers with thickness ranging from 20 to 140 μm are laminated together with platinum (Pt) inner electrodes. The growth of Bi_2O_3-doped ZnO grains within a very limited space between Pt electrodes is investigated. The grain growth behavior outside the confinement of electrodes is also studied for comparison purposes. At the beginning of sintering, a similar grain growth behavior is observed at different locations of the laminated structure. However, as sintering proceeds, the rate of grain growth within the Pt inner electrodes is decreased because of the decrease of available transportation paths. The grains between the electrodes then develop into a columnar shape as they make contact with the electrodes above and below them. Both the grain size and its distribution decrease with decreasing layer thickness.

I. Introduction

With the advance of tape-casting technologies, many electronic components are now present in a multilayered structure. Similar to bulk ceramics, the performance of laminated components also depends strongly on its microstructure. Among all the microstructure characteristics, grain size is one of the most important parameters to determine the performance of ceramics. Prevention of grain growth during sintering is a topic that has thus attracted considerable attention.

The grain growth behavior within a very small space may be different from that of bulk material. For example, grain growth behavior in a thin film is considerably different from that in bulk material.[1] Thompson indicated that normal grain growth occurs as the size of grains is smaller than the film thickness. A columnar grain structure then develops as grains intersect the surfaces of the film. Abnormal grain growth takes place after the columnar structure is formed.

The grain growth behavior of a ceramic layer within a laminated structure may also be affected by the presence of inner electrodes. However, to our surprise, the grain growth behavior within a laminated structure has attracted much less attention. In the present study, the grain growth behavior of ceramic grains within metallic electrodes is investigated.

A Bi_2O_3-doped zinc oxide (ZnO) system is chosen as the ceramic phase in the present study. The grain growth behavior of Bi_2O_3-doped ZnO has been well documented.[2–4] The previous studies investigated mainly grain growth behavior in bulk specimens. The growth of ZnO grains in bulk specimens is relatively free from any physical constraints. Nowadays, most passive components are in the form of a multilayered structure. In order to increase the volume efficiency, the layer thickness is decreased from tenths of micrometers to several micrometers. The grain growth behavior within a limited volume is a topic of increasing technological importance.

Owing to the unique grain boundary effect, ZnO-based oxides have been widely used for protecting electronic devices against voltage surges.[5–8] Because the voltage used in the current 3C appliances is low, multilayer varistors (MLV) with thin ZnO-based layers have been developed. The electrostatic barrier induced by one Bi_2O_3-rich grain boundary is approximately a constant, 3.5 V.[7] As an electric field is applied, the electrical current tends to pass through the weakest part, the part with the smallest number of grains within inner electrodes. Therefore, the extent of size variation dominates the electrical breakdown behavior. Reducing the grain size distribution is thus critical to the performance of MLV. One unique advantage of using the Bi_2O_3-doped ZnO system is that the size variation of the Bi_2O_3-doped ZnO grains can be easily monitored through the electrical measurement. The multilayer structure with the ceramic part of Bi_2O_3-doped ZnO can serve as a model system to investigate grain growth behavior within a multilayered structure. To avoid the complexity involved with the interactions between the ceramic and the electrode, a chemically inert metal, platinum (Pt), is used as the electrode material in the present study.

II. Experimental Procedure

A solvent-based slurry of ZnO and 5 wt% Bi_2O_3 was prepared first. A tape with a thickness of 20 μm was then cast. A Pt paste was deposited onto an unfired (green) tape by screen printing. In order to evaluate the effect of thickness on the grain growth behavior, a multilayer structure with various thicknesses from 20 to 140 μm was prepared by laminating different numbers of green tapes. To facilitate comparison, the layers with different thickness were all built into one component. The cross section of one typical specimen is shown in Fig. 1. The laminates were then cut into a size of 1.85 mm (length) × 0.95 mm (width) × 0.75 mm (thickness). All specimens were firstly fired from room temperature to 400°C in air for 1 h at a heating rate of 1°C/min to remove the organics. After the burnout stage, sintering was performed in air at 900°–1200°C for various durations of time, with heating and cooling rates of 5°C/min. Most specimens were prepared by sintering at 1100°C unless otherwise stated. In order to limit the evaporation of Bi_2O_3 during sintering, a powder bed with the same composition as that of the specimen was used to cover the specimens.[9,10]

For microstructure observation, the specimens were ground with SiC abrasive papers and polished with Al_2O_3 particles. The specimens were etched with dilute hydrochloric acid. The microstructures were observed using field-emission scanning electron

L. Klein—contributing editor

Manuscript No. 23226. Received May 18, 2007; approved October 26, 2007.
*Member, the American Ceramic Society.
This work was financially supported by the National Science Council, Taiwan, through the contract number of NSC95-2221-E-002-083.
†Author to whom correspondence should be addressed. e-mail: tuan@ccms.ntu.edu.tw

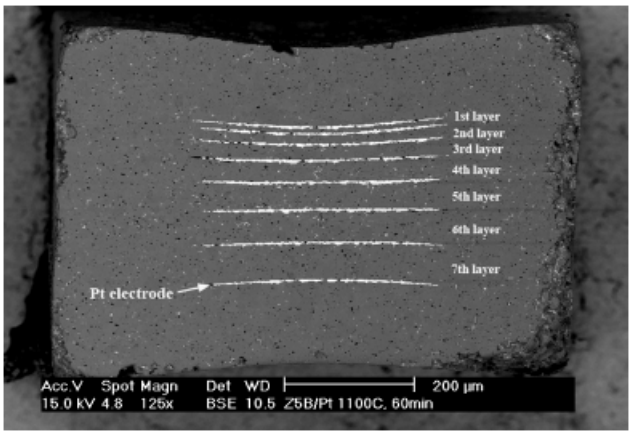

Fig. 1. Cross section of a laminated specimen used in the present study. Seven layers with different thickness are denoted as the 1st to the 7th layer.

microscopy (FE-SEM, Leo 1530, Philips Co., Eindhoven, the Netherlands). An image analysis technique was carried out to determine the area of each grain. The area was then transformed into grain diameter by assuming that the grains are spherical in shape, although it might not be the case as the sintering time was long. Over 200 grains were measured for each specimen. Electron backscatter diffraction (EBSD, TSL Co., Tokyo, Japan) patterns were also taken during FE-SEM observation to identify the texture of each ceramic layer. A tilt of 70° was used to obtain the EBSD patterns.

III. Results

Figure 1 shows the cross section of a typical multilayer structure used in the present study. The multilayer structure is composed of seven Bi_2O_3-doped ZnO layers and Pt inner electrodes. The thickness of the Bi_2O_3-doped ZnO layers varies from 8 to 55 μm after sintering at 1100°C for 1 h. These layers from the thinnest to the thickest layers are denoted as the 1st to the 7th layer as shown in Fig. 1.

The microstructure of the area outside the inner electrodes is taken as the reference to the grain growth behavior constrained by the inner electrodes. Figure 2 shows the typical micrographs of the Bi_2O_3-doped ZnO grains outside the Pt electrodes after

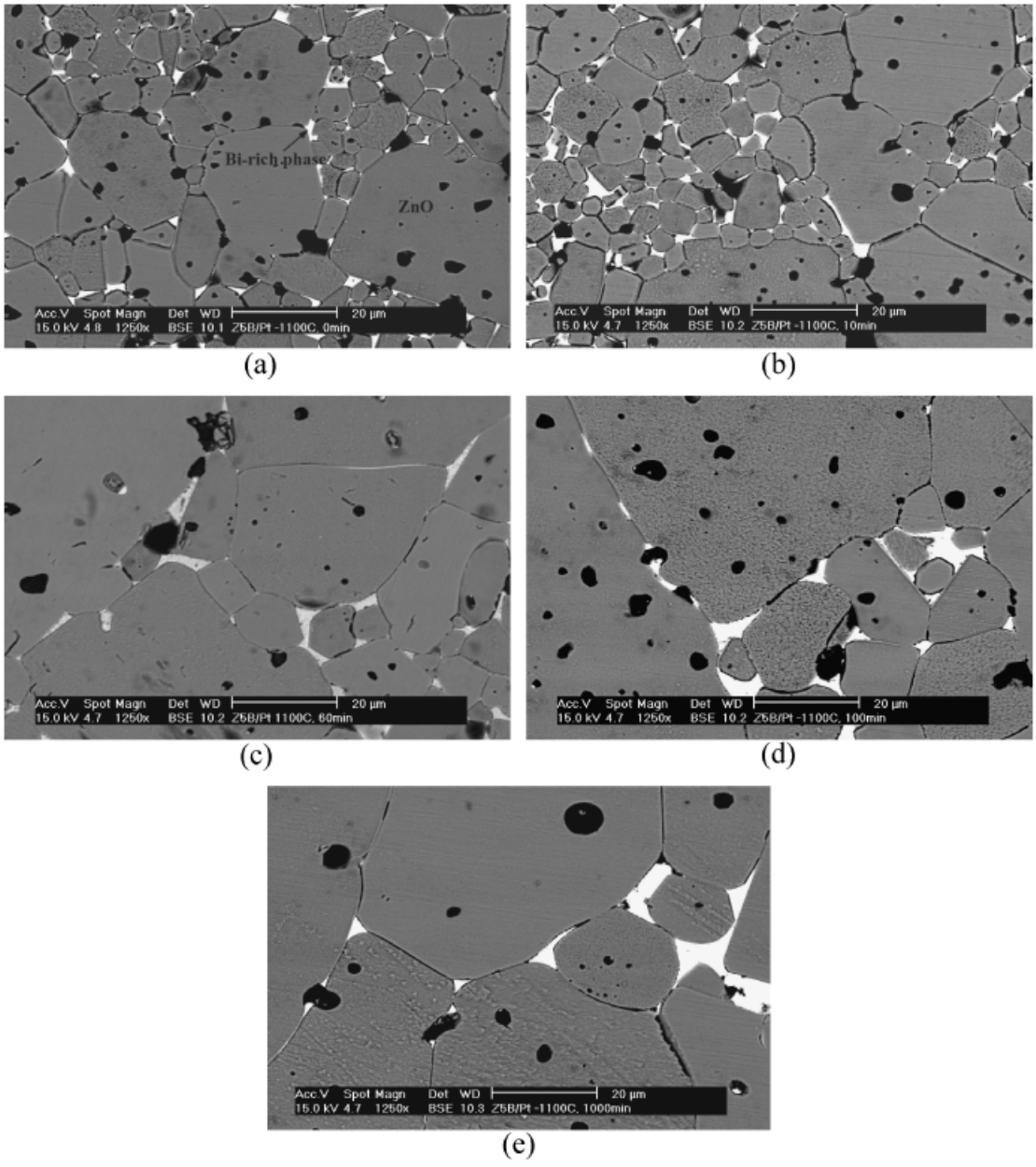

Fig. 2. Typical micrographs of the outside electrode area. The specimens were sintered at 1100°C for (a) 0, (b) 10, (c) 60, (d) 100, and (e) 1000 min.

sintering at 1100°C for 0, 10, 60, 100, and 1000 min. In the figures, the white phase shows the Bi_2O_3-rich liquid phase, the gray phase shows ZnO, and the black phase shows a pore. The Bi_2O_3-rich liquid phase is mainly located at the grain boundaries or in the triple junctions.[11–13] The pores are found in all the specimens, usually at grain boundaries and triple junctions. Many pores are also found trapped within the ZnO grains, which was attributed to the high dihedral angle and high grain boundary mobility.[14] The sizes of ZnO grains and pores all increase with increasing sintering time. Furthermore, some abnormal grains with a size more than two times that of the average grain size are found.

Figure 3 shows the typical micrographs of the thickest layer, the 7th layer, after sintering. The microstructure of this layer is more or less the same as that outside the electrodes. Many trapped pores and some abnormal grains are also found. Typical micrographs of the 1st, 2nd, and 3rd layers within the Pt electrodes are shown in Fig. 4. Similar to the microstructure outside the Pt electrodes, ZnO grains, Bi_2O_3-rich boundary phases, and pores are all found. However, different from the microstructure outside the electrodes and of the 7th layer, trapped pores (within ZnO grains) and abnormal ZnO grains are seldom found in these three layers. From Figs. 3 and 4, it can be seen that the size of ZnO grains decreases with the decrease of layer thickness. Although the growth of ZnO grains parallel to the electrodes is still possible, the ZnO grains can no longer grow in the direction perpendicular to the Pt electrodes after prolonged sintering. As the sintering time increases to 100 min, the grain boundaries tend to intersect with the inner electrodes, and columnar ZnO grains start to form. The formation of columnar grains occurs with their longer dimensions parallel to the Pt electrodes, indicating that the growth of ZnO grains is constrained by the presence of inner electrodes.

Figure 5 shows the size of ZnO grains in each layer as a function of time. The size of the ZnO grains outside the Pt electrodes is also shown for comparison. The coarsening of ZnO grains is very quick in the period from 0 min to 60 min, irrespective of whether they are outside or within the Pt electrodes. As the dwell time is longer than 60 min, the ZnO grains outside the electrodes keep growing gradually compared with those in the 1st to 3rd layers within the electrodes. At any specific time, the size of ZnO grains decreases with a decrease in the layer thickness. Furthermore, a plateau is reached as the size of grains approaches their layer thickness. This indicates that the size of ZnO grains is limited by the space available between the inner electrodes.

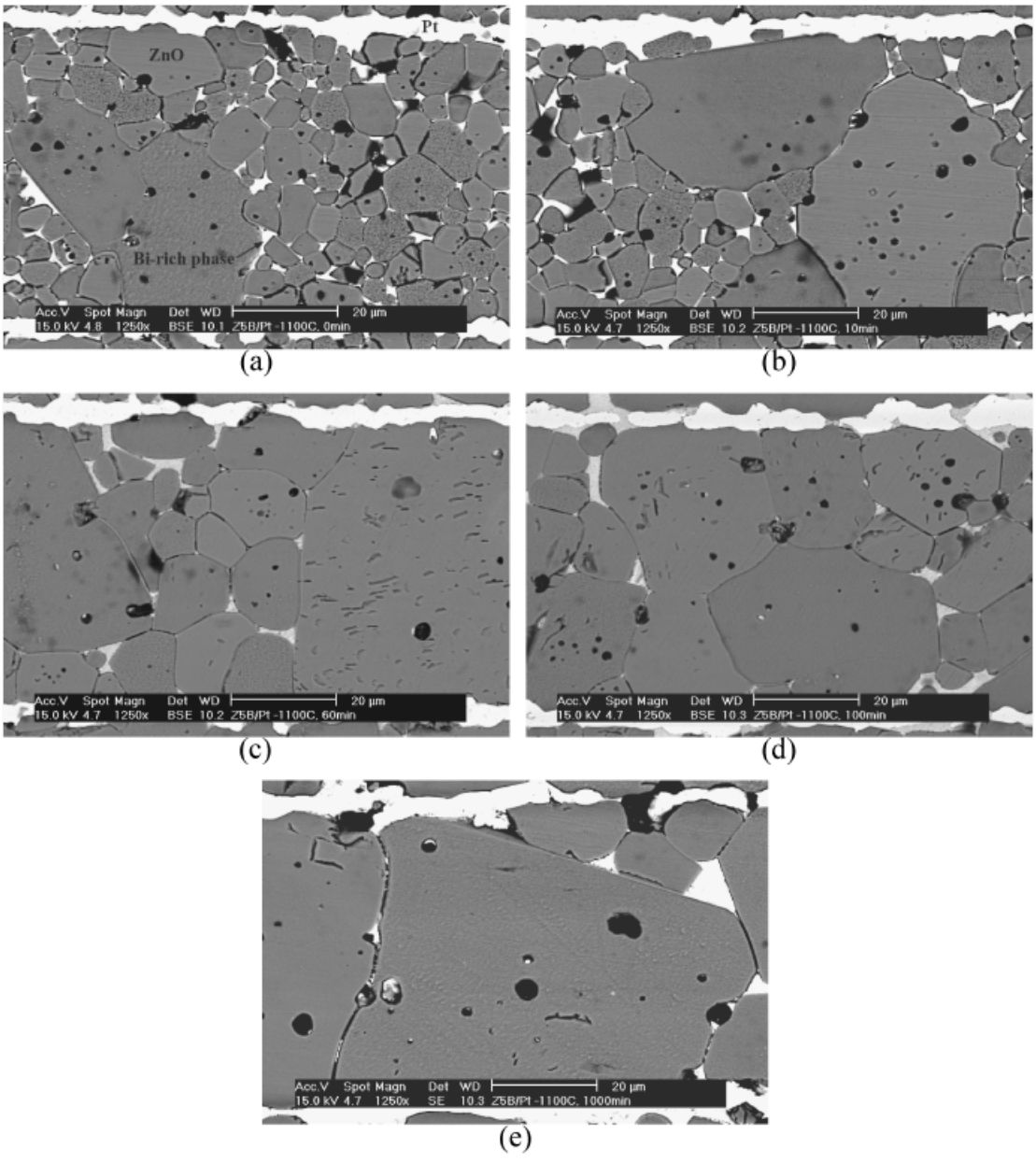

Fig. 3. Typical micrographs of the 7th layer. The specimens were sintered at 1100°C for (a) 0, (b) 10, (c) 60, (d) 100, and (e) 1000 min.

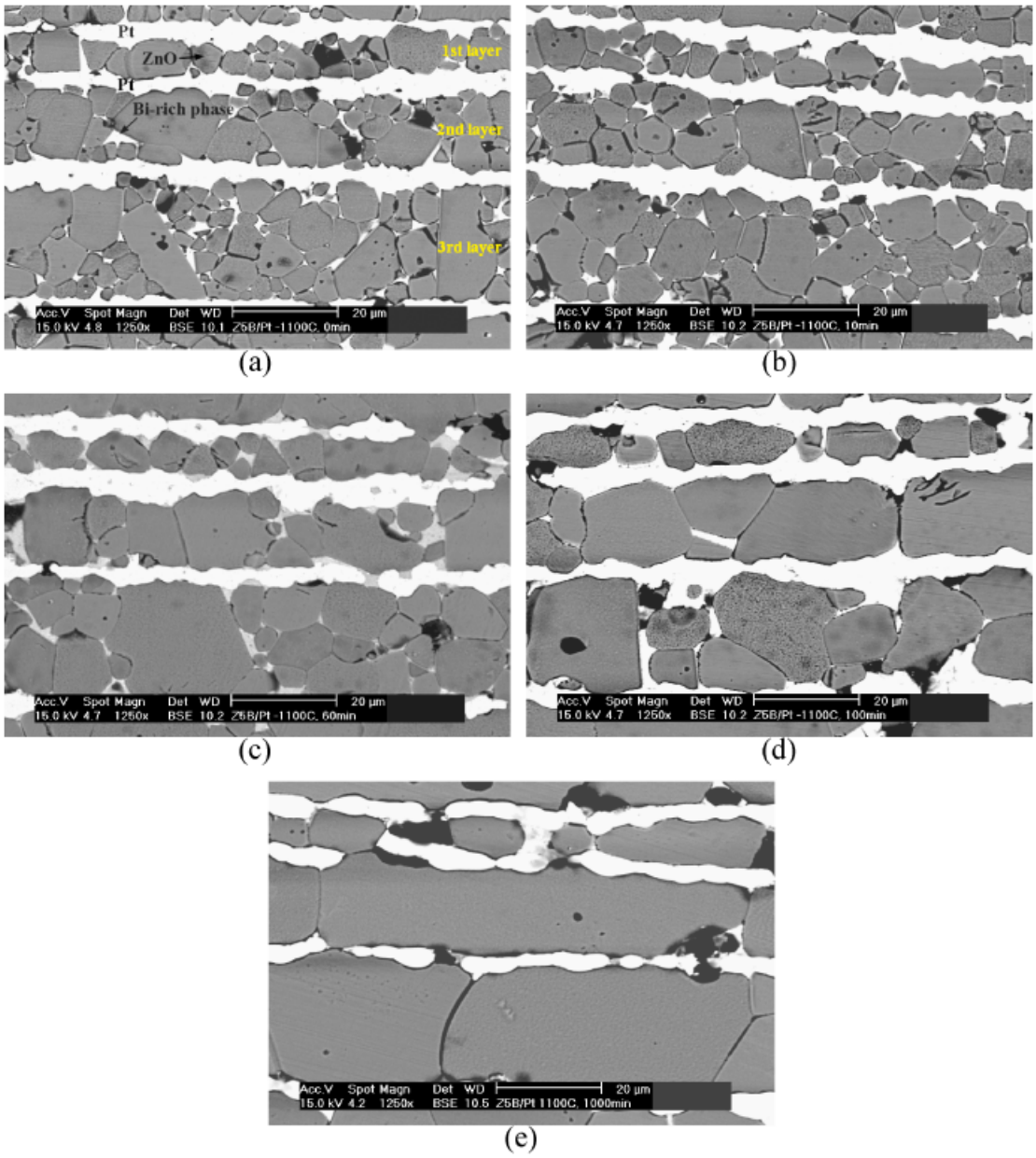

Fig. 4. Typical micrographs of the 1st to 3rd layers. The specimens were sintered at 1100°C for (a) 0, (b) 10, (c) 60, (d) 100, and (e) 1000 min.

Grain growth is a thermally activated process; its kinetics can usually be expressed as a function of temperature, T, as[3]

$$G^n = K_0 t \exp(-Q/RT) \tag{1}$$

where G is the average grain size at time t, the value of n is the kinetic grain growth exponent, K_0 is a constant, Q is the apparent activation energy, and R is the gas constant. Equation (1) can be rewritten as

$$\log(G^n/t) = \log K_0 - 0.434Q/RT \tag{2}$$

Because

$$\log G = (1/n)\log t + (1/n)(\log K_0 - 0.434Q/RT) \tag{3}$$

The grain growth exponent, n, can thus be calculated from the slope of the log (grain size) versus log (time) plots, Fig. 5. The n value for the growth of ZnO grains in the outside electrode area is around 3. The grains within the electrodes follow the same trend as those in the outside area in the beginning of

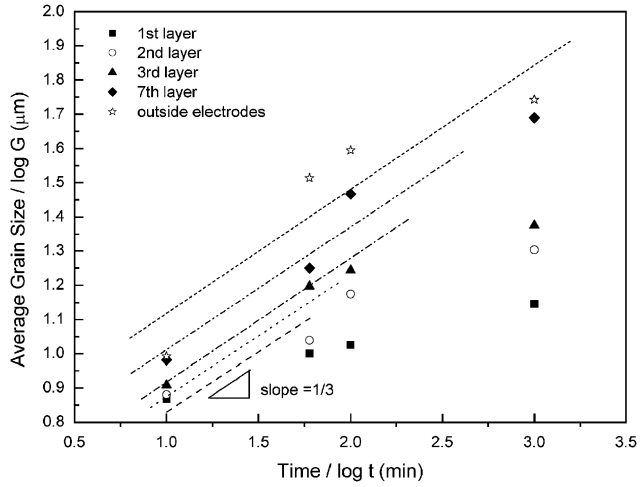

Fig. 5. Average size of Bi_2O_3-doped zinc oxide grains as a function of dwell time at 1100°C.

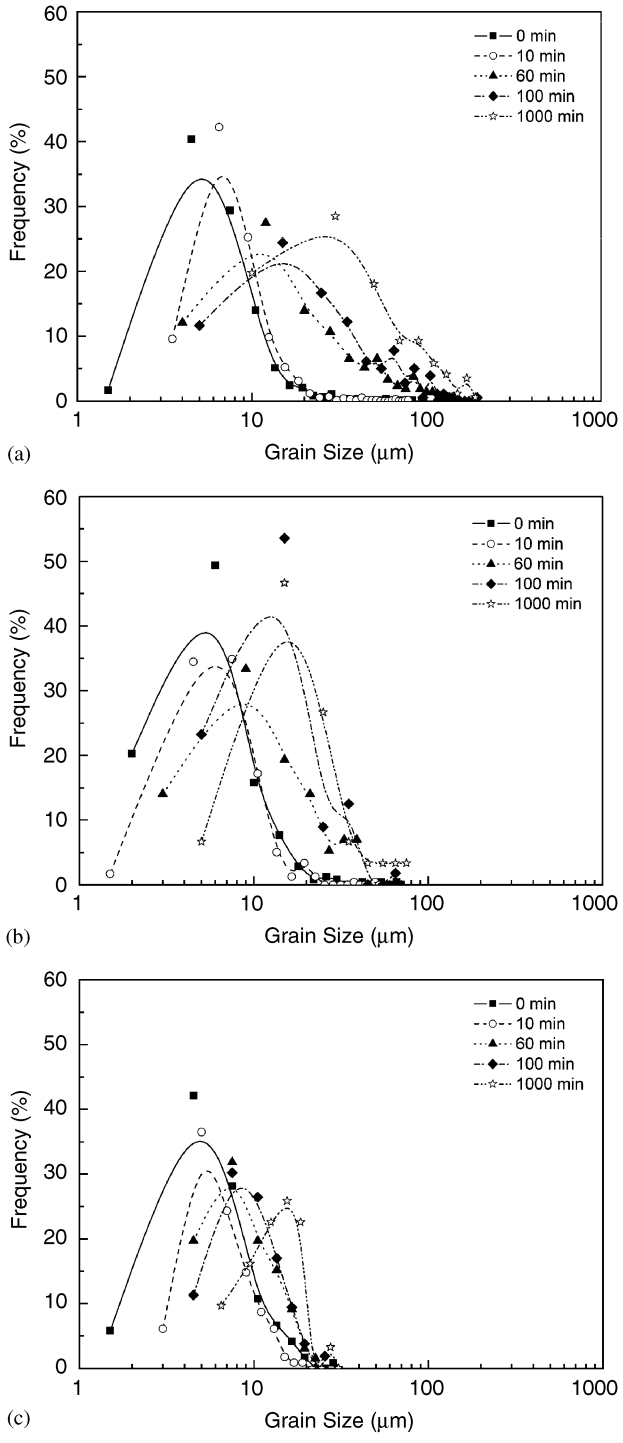

Fig. 6. Size distribution of the zinc oxide grains (a) outside the electrode area, (b) within the 3rd layer, and (c) within the 1st layer. The specimens were sintered at 1100°C.

sintering. Then, the grain growth within electrodes is significantly slowed down as the size of the grains approaches the layer thickness. After knowing the value of n, the activation energy, Q, for the grain growth within the temperatures range from 900° to 1200°C can be calculated. For the grain growth in the outside electrode area, the calculated activation energy is 381 kJ/mol.

The size distribution of the ZnO grains outside and within Pt electrodes is shown in Fig. 6. The vertical axis in the figure displays the number frequency. For the ZnO grains in the outside area, Fig. 6(a), the size distribution exhibits a typical lognormal distribution throughout the firing cycle. The frequency peak moves toward its right-hand side with an increase of dwell time. For the grains at the 3rd layer, Fig. 6(b), although the frequency

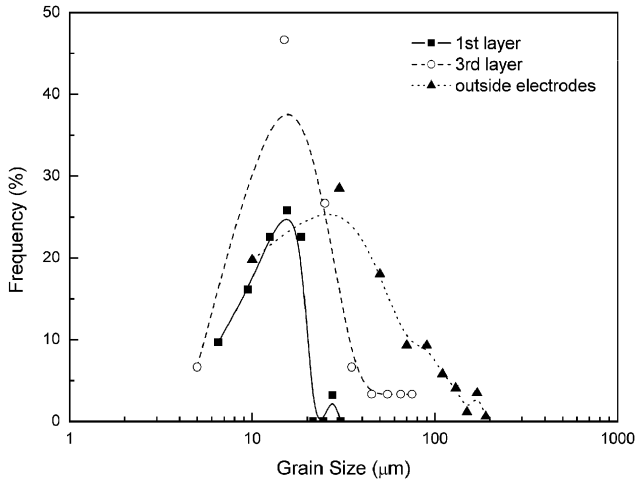

Fig. 7. Size distribution of zinc oxide grains in the outside electrode area and within the 1st and 3rd layers. The specimen was sintered at 1100°C for 1000 min.

peak of the ZnO grains within Pt electrodes also moves to its right-hand side, the size scatter is narrower compared with that in the outside area. For the grains in the thinnest layer (1st layer, Fig. 6(c)), the frequency peak moves much slower toward its right-hand side. It is also worth noting that the ZnO grains in the specimen sintered at 1100°C for 1000 min no longer follow the lognormal distribution. The large grains in the distribution curve seem to be chopped off from the curve. Only the grains below a certain size are present. To facilitate comparison, the size distribution curves for the ZnO grains in the 1st, 3rd, and outside electrode area are shown in Fig. 7. Although all the grains are within one multilayer specimen, the average size and size scatter depend strongly on their locations. The figure demonstrates that the size variation is decreasing with a decrease of the layer thickness.

Figure 8 shows the EBSD patterns of the 1st to the 3rd layer after sintering at 1100°C for 0, 60, and 1000 min. A portion of the outside electrode area is also shown for comparison. The size of the mapping area is nearly the same for all three specimens. In Figs. 8(b), (d), and (f), each color represents one orientation that corresponds to the color-inverse pole figure as shown in Fig. 8(g). The figure indicates that the electrodes are polycrystalline in nature after firing. Because the EBSD technique is very sensitive to the flatness of the detected area, it is not possible to determine the size of Pt grains due to lack of flatness. As the dwell time at 1100°C is shorter than 100 min, the orientation of ZnO grains is randomly distributed. As the dwell time increases to 1000 min, the grains in the 1st layer tend to rotate to $(10\bar{1}0)$and $(2\bar{1}\bar{1}0)$ planes; the grains in the 2nd and 3rd layers tend to rotate to the (0001) plane. In general, no consistent preferred orientation throughout the multilayer structure is observed.

The breakdown voltage of the multilayer specimens is shown as a function of dwell time in Fig. 9. The breakdown voltage is around 1.5 V for the specimens sintered at 1100°C for <100 min, and then declines to nearly zero as the dwell time increases to 1000 min.

IV. Discussion

A novel design on a laminated structure is used in the present study. Seven layers with different thicknesses are incorporated into one multilayer structure. The metallic Pt is chemically inert to ZnO and bismuth oxide. The growth of ZnO grains within the electrodes is constrained due to the presence of Pt inner electrodes. Therefore, the Pt electrodes can be seen as a physical barrier to the growth of ZnO grains. Through careful microstructure characterization, the following observations can be made:

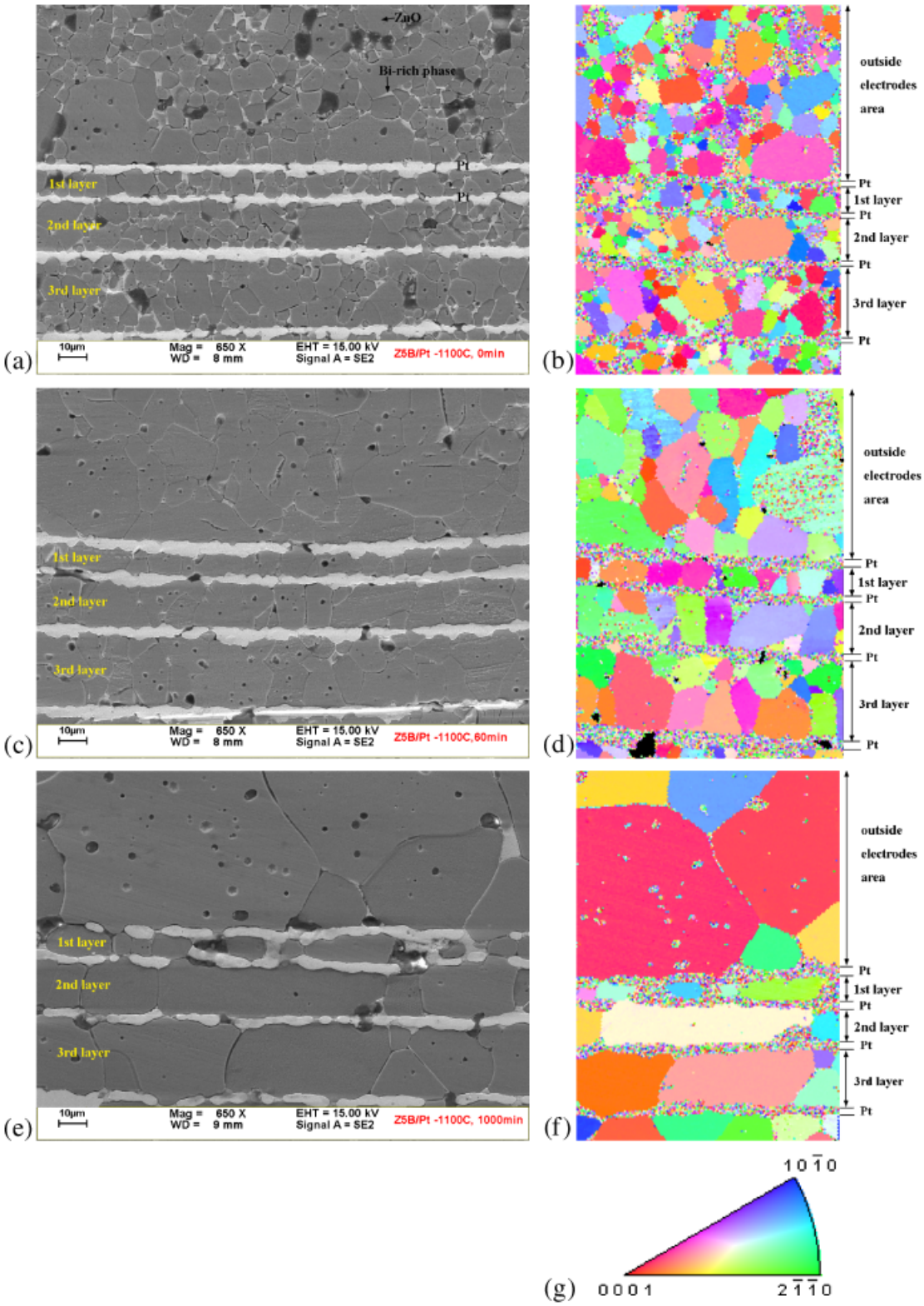

Fig. 8. Scanning electron micrographs and their corresponding electron back scatter diffraction patterns for the specimens sintered at 1100°C for (a), (b) 0 min, (c), (d) 60 min, and (e), (f) 1000 min. The inverse pole figure is shown in (g).

(1) At the beginning of sintering, a similar grain growth behavior is observed at different locations of the laminated structure.

(2) As ZnO grains intersect the top and bottom electrodes, the growth of grains is possible only in the direction parallel to the electrodes.

(3) As the size of grains approaches the layer thickness, the grain boundaries tend to become perpendicular to the electrode and develop into a columnar shape.

(4) The average size of ZnO grains decreases with a decrease of the layer thickness.

(5) The extent of size variation also decreases with decreasing layer thickness.

(6) No preferred orientation is developed throughout the laminated structure after prolonged sintering.

In the present study, the area outside the electrodes is taken as the reference. The space outside the electrodes, $\sim$200 μm wide,

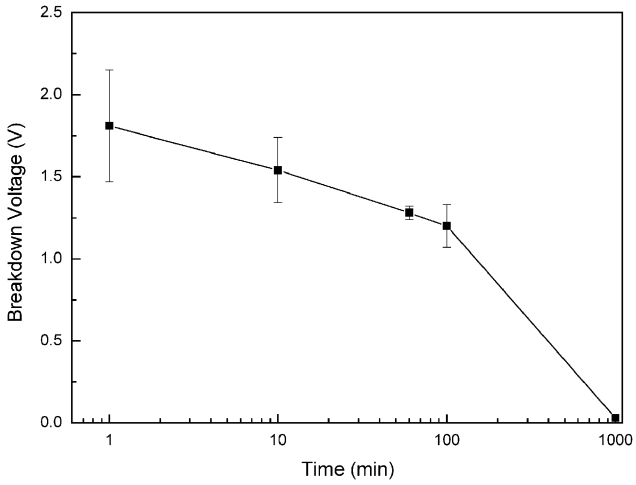

Fig. 9. Breakdown voltage of the laminated specimens sintered at 1100°C for 0, 10, 60, 100, and 1000 min.

is much larger than that within the electrode. The grains can thus grow rather freely in this area. However, it is worth noting that as the size of the grains is close to the space available in the outside area, say 50 μm, the free surface may also exert a constraint on the growth of ZnO grains. It can thus be found from Fig. 5 that the size of ZnO grains in the outside electrode area in the specimen sintered for 1000 min is smaller than the values extrapolated from the shorter times. As long as the dwell time is shorter than 1000 min, the grain growth behavior in the outside electrode area can still be treated as a basis for comparison.

Some large ZnO grains are easily found in the outside area and in the thick ZnO layers; see Figs. 2 and 3. The formation of these abnormal grains may be related to the large particles in the starting powder or the nonuniform distribution of a Bi_2O_3-rich liquid phase. The average size, d_{50}, of the starting ZnO particles is 1.2 μm; d_{10} and d_{90} are 0.5 and 2.9 μm, respectively. The size distribution of the starting ZnO particles is not wide. Therefore, the formation of abnormal grains more likely resulted from the nondistribution of the Bi_2O_3-rich liquid phase. One may note that the shrinkage in the middle of the laminated structure is much larger than the other parts of the structure; see Fig. 1. As will be demonstrated later, Bi_2O_3-rich liquid tends to remain closer to ZnO grains than to Pt electrodes. Owing to the presence of Pt electrodes, the distribution of the Bi_2O_3-rich liquid may not be uniform after the formation of the liquid, which is around 825°C.[2,15]

The grain growth exponent n and activation energy Q for the growth of ZnO grains in the outside area are 3 and 381 kJ/mol, respectively. Dey and Bradt[2] had carried out their study on the bulk ZnO–Bi_2O_3 specimens containing 3–12 wt% Bi_2O_3. The reported n value for Bi_2O_3-containing ZnO was 5. From the Fig. 5 in their paper, the activation energy for the ZnO-5 wt% Bi_2O_3 can be estimated by applying the extrapolation technique. The estimated activation energy for the ZnO-5 wt% Bi_2O_3 is around 200 kJ/mol. Our experimental values are different from theirs. The difference may be related to the limited space available for the growth of ZnO grains in the laminated specimens used in the present study. However, the present authors highly suspect that the embedding powder may also play a key role in such difference. In the present study, a considerable amount of the same ZnO–Bi_2O_3 powder mixtures is used as a powder bed to avoid evaporation of Bi_2O_3, which also starts as early as 825°C.[9,10,15] As indicated in the study of Dey and Bradt,[2] the increase of the Bi_2O_3-rich liquid increases the activation energy of the grain growth of ZnO grains. Because the remaining Bi_2O_3-rich liquid is high due to the use of a powder bed in the present study, the activation energy is thus higher. As suggested by Dey and Bradt[2], the growth of ZnO grains used in the present study is also likely controlled by diffusion through the liquid phase.

In the beginning of sintering, the Bi_2O_3 is melted at a temperature as low as 825°C.[2,15] The Bi_2O_3-rich liquid phase remains at the grain boundaries throughout the whole firing process due to the presence of a protective powder bed. The mass transportation through the liquid phase induces densification as well as grain growth. Before ZnO grains touch the upper and bottom electrodes, a similar grain growth is observed in the area outside and within the electrodes. The slope for the grain growth kinetics for all the layers equals 1/3 as revealed in Fig. 5. However, as the size of ZnO grains approaches the layer thickness, the growth of ZnO grains is constrained by the limited space available for their growth. The growth thus slows down significantly. The slopes in Fig. 5 for the 1st to 3rd layers are less than 1/3 as the sintering time is long.

The grain growth can be seen as the movement of grain boundary as[16]

$$v = \beta MF \tag{4}$$

where v is the velocity of the grain boundary movement, β is the geometric factor that depends on the routes available for the mass flow (see Fig. 10), F is the force, and M is the intrinsic mobility of the boundary. The force, F, on the grain boundary is controlled by the curvature of grains as

$$F = \frac{\bar{\gamma}_{gb}}{\overline{G}} \tag{5}$$

where $\overline{G}$ is the average grain size and $\bar{\gamma}_{gb}$ is the average grain boundary energy per unit area of grain boundary. The mobility of the grain boundary is controlled by the diffusion through the liquid phase. Because the liquid remains throughout the sintering, the M can be treated as a constant. At the beginning of sintering, the routes available for mass transportation at different locations in a multilayer structure are the same. The slopes of all layers equal 1/3. A similar grain growth kinetic is found for different locations of the multilayer structure. However, the mass transportation paths available in the limited space between inner electrodes are reduced when the ZnO grains touch the upper and bottom electrodes. This results in the reduction of the value of β (Eq. (4)). The slopes of the 1st, 2nd, or 3rd layer thus decrease.

There is no texture observed in the laminated structure at least within the timeframe of 1000 min. Different from the growth of grains in a thin film, the substrate for the thin film

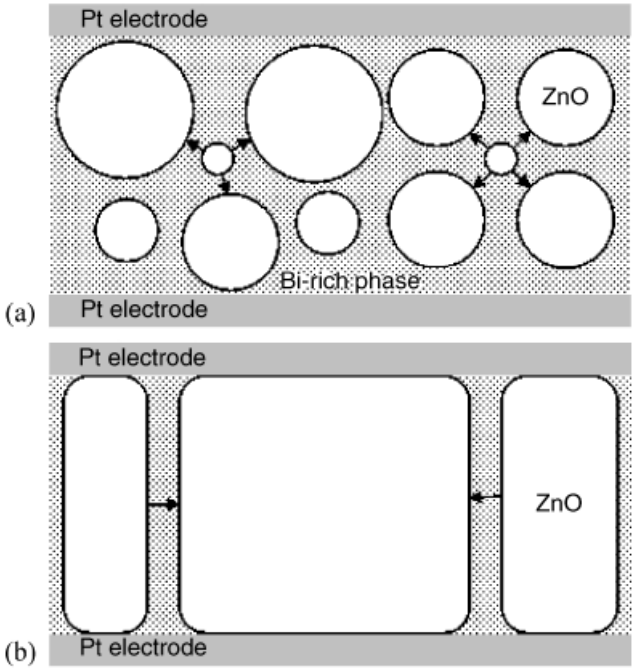

Fig. 10. Schematics of the growth of zinc oxide grains (a) in the beginning of sintering and (b) after prolonged sintering within Pt electrodes.

is usually a single crystal or a layer with only one orientation. The growth of the grains is affected by the orientation of the bottom layer; a preferred orientation is frequently induced. However, the Pt electrode prepared by screen printing of fine Pt particles is polycrystalline after sintering. Owing to this polycrystalline nature, it is difficult to induce a preferred orientation for the thin layers.

After the columnar structure is developed in a thin film, abnormal grain growth is triggered due to the low interface energy between the film and the substrate.[1] However, for the system investigated in the present study, the ZnO–Bi_2O_3 interface energy is the lowest. Chiang had investigated the ZnO–Bi_2O_3 system through the use of high-resolution transmission electron microscopy.[17] A very thin Bi_2O_3 layer, with a thickness of 1.0–1.5 nm, is always present between ZnO–ZnO grains. They thus proposed that the ZnO–Bi_2O_3 interface energy is low. The low interface energy can also be confirmed using the electrical measurement as shown in Fig. 9. The breakdown voltage of one Bi_2O_3-rich boundary layer is around 1.5 V.[18] Figure 9 indicates that there are only one to two Bi_2O_3-rich boundaries present at a certain place within Pt electrodes after sintering for a very short time at 1100°C. As long as there is one large grain approaching the layer thickness, the electrical breakdown is then determined by the very large grain. It thus demonstrates that the grain size distribution is wide in the beginning of sintering. As the dwell time increases to 1000 min, no Bi_2O_3-rich boundary exists between Pt and ZnO, and in at least some parts of the Pt–ZnO interface, the laminated specimen transforms into a semiconductor as that of ZnO. It demonstrates that the ZnO–Bi_2O_3 interface energy is lower than that of the ZnO–Pt interface. Owing to the low energy of the ZnO–Bi_2O_3 interface, abnormal grain growth is not preferred. The diffusion path available decreases with the increase of grain size; the growth of large ZnO grains is thus constrained. The ones with a size smaller than the layer thickness can nevertheless grow. Therefore, a uniform microstructure is developed in the laminated structure.

V. Conclusions

Grain growth behavior within a very small space between inert electrodes is investigated in the present study. As long as the inner electrode is chemically inert to the ceramic layer, the growth of ceramic grains is constrained by the inner electrodes. The growth of ZnO grains within the Pt inner electrodes is prohibited due to the decrease of the transportation paths available. Not only is the average size reduced by the decreasing layer thickness; the size variation is also decreased. A uniform microstructure is therefore developed within the laminated structure. Owing to the polycrystalline nature of the inner electrode, no texture is developed in the laminated structure.

References

[1]C. V. Thompson, "Grain Growth in Thin Film," *Annu. Rev. Mater. Sci.*, **20**, 245–68 (1990).

[2]D. Dey and R. C. Bradt, "Grain Growth of ZnO during Bi_2O_3 Liquid-Phase Sintering," *J. Am. Ceram. Soc.*, **75** [9] 2529–34 (1992).

[3]T. Senda and R. C. Bradt, "Grain Growth in Sintered ZnO and ZnO–Bi_2O_3 Ceramics," *J. Am. Ceram. Soc.*, **73** [1] 106–14 (1990).

[4]V. Gunay, O. Gelecek-Sulan, and O. T. Ozkan, "Grain Growth Kinetic in xCoO–6 wt% Bi_2O_3–(94−x) ZnO (x = 0, 2, 4) Ceramic System," *Ceram. Int.*, **30**, 105–10 (2004).

[5]L. M. Levinsion and H. R. Philipp, "Zinc Oxide Varistors—A Review," *Am. Ceram. Soc. Bull.*, **65** [4] 639–49 (1986).

[6]T. K. Gupta, "Application of Zinc Oxide Varistors," *J. Am. Ceram. Soc.*, **73** [7] 1817–40 (1990).

[7]D. R. Clarke, "Varistor Ceramics," *J. Am. Ceram. Soc.*, **82** [3] 485–502 (1999).

[8]J. Cai, Y. H. Lin, M. Li, C. W. Nan, J. He, and F. Yuan, "Sintering Temperature Dependence of Grain Boundary Resistivity in a Rare-Earth-Doped ZnO Varistor," *J. Am. Ceram. Soc.*, **90** [1] 291–4 (2007).

[9]G. Y. Sung, C. H. Kim, and M. H. Oh, "Effect of Grain-Size Distribution on the Barrier Voltage of ZnO Varistors," *Adv. Ceram. Mater.*, **2** [4] 841–7 (1987).

[10]G. C. Miles and A. R. West, "Pyrochlore Phase in the System ZnO–Bi_2O_3–Sb_2O_3: I. Stoichiometries and Phase Equilibria," *J. Am. Ceram. Soc.*, **89** [3] 1042–6 (2006).

[11]J. Wong and W. G. Morris, "Microstructure and Phases in Nonohmic ZnO–Bi_2O_3 Ceramics," *Am. Ceram. Soc. Bull.*, **53** [11] 816–20 (1974).

[12]W. D. Kingery, J. B. Vander Sande, and T. Mitamura, "A Scanning Transmission Electron Microscopy Investigation of Grain-Boundary Segregation in a ZnO–Bi_2O_3 Varistor," *J. Am. Ceram. Soc.*, **62** [3–4] 221–2 (1979).

[13]H. Cerva and W. Russwurm, "Microstructure and Crystal Structure of Bismuth Oxide Phases in Zinc Oxide Varistor Ceramics," *J. Am. Ceram. Soc.*, **71** [7] 522–30 (1988).

[14]J. H. Choi, N. M. Hwang, and D. Y. Kim, "Pore-Boundary Separation Behavior during Sintering of Pure and Bi_2O_3-Doped ZnO Ceramics," *J. Am. Ceram. Soc.*, **84** [6] 1398–400 (2001).

[15]E. M. Levin, C. R. Robbins, and H. F. McMurdiein, *"Metal Oxide Systems," Phase Diagrams for Ceramists*, Vol.1, Edited by M. K. Reser. American Ceramic Society, Columbus, OH, 1964; p. 126.

[16]R. J. Brook *"Controlled Grain Growth," Treatise on Materials Science and Technology*, Vol. 9, Edited by F. F. Y. Wang. Academic Press Inc, New York, NY, 1976; p. 331.

[17]H. Wang and Y. M. Chiang, "Thermodynamic Stability of Intergranular Amorphous Films in Bismuth-Doped Zinc Oxide," *J. Am. Ceram. Soc.*, **81** [1] 89–96 (1998).

[18]Y. W. Lao and W. H. Tuan, "Effects of Bi_2O_3 and Sb_2O_3 on the Microstructure and Electrical Properties of ZnO Varistors"; to be published. □